Protein-Based Thermoplastic Elastomers

Karthik Nagapudi,[†] William T. Brinkman,[†] Johannes Leisen,[‡] Benjamin S. Thomas,[†] Elizabeth R. Wright,[§] Carolyn Haller,[†] Xiaoyi Wu,[†] Robert P. Apkarian,[§,⊥] Vincent P. Conticello,[§] and Elliot L. Chaikof*[,†,#]

Departments of Surgery and Biomedical Engineering, Emory University School of Medicine and Georgia Institute of Technology, Atlanta, Georgia 30332; School of Polymer, Textile, and Fiber Engineering, Georgia Institute of Technology, Atlanta, Georgia 30322; Department of Chemistry, Emory University, Atlanta, Georgia 30332; Integrated Microscopy & Microanalytical Facility, Emory University, Atlanta, Georgia 30332; and School of Chemical and Biomolecular Engineering, Georgia Institute of Technology, Atlanta, Georgia 30322

Received May 5, 2004; Revised Manuscript Received September 18, 2004

ABSTRACT: Investigations of high molecular weight recombinant protein triblock copolymers demonstrate unique opportunities to systematically modify material microstructure on both nano- and meso-length scales in a manner not been previously demonstrated for protein polymer systems. Significantly, through the biosynthesis of BAB-type copolymers containing flanking, plastic-like end blocks and an elastomeric midblock, virtually cross-linked protein-based materials were generated that exhibit tunable properties in a manner completely analogous to synthetic thermoplastic elastomers. Through the rational choice of processing conditions that control meso- and nanoscale structure, changes of greater than 3 orders of magnitude in Young's modulus (0.03−35 MPa) and 5-fold in elongation to break (250−1300%) were observed. Extensibility of this range or magnitude has not been previously reported for virtually cross-linked copolymers that have been produced by either chemical or biosynthetic approaches. We anticipate that these versatile protein-based thermoplastic elastomers will find applications as novel scaffolds for tissue engineering and as new biomaterials for controlled drug release and cell encapsulation.

Introduction

The emergence of genetic engineering of synthetic polypeptides has recently enabled the preparation of multiblock protein copolymers composed of complex peptide sequences in which individual blocks may have different mechanical, chemical, or biological properties.[1,2] For example, Cappello and colleagues[3] have produced a series of protein polymers ranging up to 1000 amino acids in size (∼85 kDa) that contain both silk- and elastin-mimetic sequences. Silklike regions consisting of between 12 and 48 alternating alanine and glycine residues are capable of crystallizing to form virtual cross-links between elastin-mimetic sequences comprised of repeating Val-Pro-Gly-Val-Gly pentapeptides that characteristically form short blocks of between 40 and 80 amino acids in length. Similarly, Petka et al.[2] have reported the synthesis of a 230-amino acid (22.5 kDa) recombinant protein triblock copolymer that gels in a thermally reversible manner through the association of a single 42-amino acid leucine zipper region located in flanking end blocks. As these and other studies have illustrated, multiblock recombinant protein polymers can form biphasic materials that exhibit, to varying degrees, properties of the constituent species.

In a fashion analogous to that observed for synthetic block copolymers, it is anticipated that the capacity to control both interphase mixing of incompatible blocks and microstructure on both nano- and meso-length scales will be important variables in tuning material properties of protein-based block copolymers. Biphasic properties are often retained for synthetic polymers, such as the segmented polyurethanes, that are formulated from small blocks. However, a large body of studies has demonstrated that the range of microstructures that can be readily accessed by multiblock copolymers is much greater for systems that are comprised of large well-defined blocks, such as the polystyrene−polybutadiene−polystyrene (SBS) or polystyrene−polyisoprene−polystyrene (SIS) copolymers.[4] Thus, approaches that facilitate the generation of large multiblock protein polymers offer a unique opportunity to systematically modify microstructure in a manner that has not been feasible in previously reported systems.

We have recently described a modular convergent biosynthetic strategy that has greatly facilitated the synthesis of high molecular weight recombinant protein triblock copolymers with significant flexibility in the selection and assembly of blocks of diverse size and structure.[5] In this report we detail the synthesis of a new class of BAB protein triblock copolymer that are derived from elastin-mimetic polypeptide sequences in which the respective blocks exhibit distinct elastomeric and plastic mechanical properties in analogy to thermoplastic elastomers. We demonstrate that by judicious selection of solution processing conditions, including solvent type, temperature, and pH, an array of virtually cross-linked protein-based materials can be produced that display a wide range of physical properties. The capacity of solution processing to modulate protein polymer behavior was attributed both to the induction of distinct highly ordered morphologies by liquid−liquid phase separation and by the control of interphase

[†] Emory University School of Medicine and Georgia Institute of Technology.
[‡] School of Polymer, Textile, and Fiber Engineering, Georgia Institute of Technology.
[§] Emory University.
[⊥] Integrated Microscopy & Microanalytical Facility, Emory University.
[#] School of Chemical and Biomolecular Engineering, Georgia Institute of Technology.
* Corresponding author: Ph (404) 727-8413; Fax (404) 727-3660; e-mail echaiko@emory.edu.

10.1021/ma0491199 CCC: $30.25
Published on Web 12/17/2004

Table 1. Coding Sequences of Oligonucleotide Cassettes Employed for the Construction of Proteins P2 and B9

A.												
Val	Pro	Gly	Val	Gly	Val	Pro	Gly	Val	Gly	Val	Pro	Gly
GTA	CCT	GGT	GTT	GGC	GTT	CCG	GGT	GTA	GGT	GTA	CCA	GGC
CAT	GGA	CCA	CAA	CCG	CAA	GGC	CCA	CAT	CCA	CAT	GGT	CCG
Glu	Gly	Val	Pro	Gly	Val	Gly	Val	Pro	Gly	Val	Gly	
GAA	GGT	GTA	CCG	GGT	GTT	GGC	GTA	CCA	GGC	GTT	GGC	
CTT	CCA	CAT	GGC	CCA	CAA	CCG	CAT	GGT	CCG	CAA	CCG	
B.												
Val	Pro	Ala	Val	Gly	Ile	Pro	Ala	Val	Gly	Ile	Pro	Ala
GTA	CCT	GCT	GTT	GGT	ATT	CCG	GCT	GTT	GGT	ATC	CCA	GCT
CAT	GGA	CGA	CAA	CCA	TAA	GGC	CGA	CAA	CCA	TAG	GGA	CGA
Val	Gly	Ile	Pro	Ala	Val	Gly	Ile	Pro	Ala	Val	Gly	
GTT	GGT	ATC	CCA	GCT	GTT	GGC	ATT	CCG	GCT	GTA	GGT	
CAA	CCA	TAG	GGA	GCA	CAA	CCG	TAA	GGC	CGA	CAT	CCA	
C.												
Met	Val	Pro	Gly	Val	Gly	Val	Pro	Gly	Val	Gly	Val	
ATG	GTT	CCG	GGT	GTA	GGT	GTA	CCT	GGT	GTT	GGG	GTA	
TAC	CAA	GGC	CCA	CAT	CCA	CAT	GGA	CCA	CAA	CCC	CAT	
Pro	Gly	Val	Gly	Ile	Pro	Ala	Val	Gly	stop	stop		
CCT	GCT	GTT	GGT	ATT	CCT	GCA	GTT	GGC	TGA	TGA		
GGA	CGA	CAA	CCA	TAA	GGA	CGT	CAA	CCG	ACT	ACT		
D.												
Met	Val	Pro	Ala	Val	Gly	Ile	Pro	Ala	Val	Gly	Val	
ATG	GTA	CCT	GCT	GTT	GGT	ATT	CCT	GCA	GTT	GGC	GTT	
TAC	CAT	GGA	CGA	CAA	CCA	TAA	GGA	CGT	CAA	CCG	CAA	
Pro	Gly	Val	Gly	Val	Pro	Gly	Val	Gly	Stop	Stop		
CCG	GGT	GTA	GGT	GTA	CCT	GGT	GTT	GGG	TGA	TGA		
GGC	CCA	CAT	CCA	CAT	GGA	CCA	CAA	CCC	ACT	ACT		

Scheme 1. Biosynthetic Route to Diblock P2 and Triblock B9 Protein Copolymers[a]

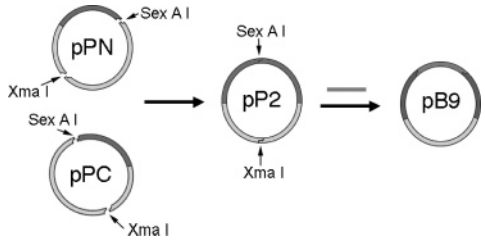

[a] DNA cassettes encoding plastic repeat units were independently synthesized and inserted into plasmids engineered as N-terminal (pPN) and C-terminal (pPC) blocks. After double digestion with *Sex* AI and *Xma* I, the two cleavage fragments are joined together via enzymatic ligation to afford plasmid pP2with a single *Sex* AI restriction site that is located between the plastic domains. After digestion of pP2 ith *Sex* AI, the elastin concatemer is ligated into pP2 to yield the triblock copolymer pB9.

mixing between incompatible blocks within the polymer-rich phase. These investigations demonstrate that the generation of large multiblock protein polymers offers a unique opportunity to systematically modify material microstructure on both nano- and meso-length scales in a manner that has not been feasible in previously reported systems. Significantly, through the rational choice of processing conditions that control meso- and nanoscale structure self-organizing protein-based materials can be produced with a variety tailored properties, including mechanical behavior and drug elution rates.

Methods

Synthesis. Synthetic methods used to produce the DNA inserts that encode the various elastin block copolymers have been described previously.[5] Oligonucleotide cassettes encoding the elastic (**A**) and plastic (**B**) repeat units (Table 1) were independently synthesized and inserted into the *Bam*H I/*Hin*D III sites within the polylinkers of pZErO-1 and pZErO-2, respectively (Scheme 1). Recombinant clones were isolated after propagation in *E. coli* strain Top10F′, double-stranded DNA sequence analysis verified the identity of the DNA inserts **A** and **B**. These clones were propagated in *E. coli* strain SCS110 in order to isolate preparative amounts of plasmid DNA. DNA monomers **A** and **B** were liberated from the respective plasmids via restriction digestion with *Bsp*M I and *Sex*A I, respectively. Self-ligation of each DNA cassette afforded a population of concatemers encoding repeats of the plastic and elastic sequences, respectively.

Concatemers derived from DNA monomer **B** were inserted into the *Bsp*M I site of the modified polylinker **C** in plasmid pET-24a. A concatemer encoding 16 repeats of the plastic sequence was isolated and identified via restriction cleavage with *Kpn* I and *Pst* I. Double-stranded DNA sequence analysis confirmed the integrity of the concatamer within the recombinant plasmid, which was labeled pPC. The concatemer was liberated from pPC via restriction cleavage with *Kpn* I and *Pst* I and purified via preparative agarose gel electrophoresis. Enzymatic ligation was used to join the concatemer cassette to the *Kpn* I/*Pst* I sites within the modified polylinker **D** in plasmid pET-24a. Double-stranded DNA sequence analysis confirmed the integrity of the concatemer within the recombinant plasmid, which was labeled pPN. The pair of recombinant plasmids pPN and pPC encoded the *N*-terminal and *C*-terminal domains, respectively, of the diblock polymer **P2**. Restriction cleavage of each plasmid with *Sex*A I and *Xma* I afforded two fragments, which were separated via preparative agarose gel electrophoresis. Enzymatic ligation of pPN and pPC afforded the recombinant plasmid pP2, which encoded protein **P2** as a single contiguous reading frame within plasmid pET-24a.

Plasmid pP2 was propagated in *E. coli* strain SCS110 and cleaved with restriction endonuclease *Sex*A I. Concatemers encoding the elastin sequence **A** were inserted into the compatible *Sex*A I site of pP2. The recombinant clones were analyzed by restriction digestion with *Kpn* I and *Pst* I, followed by agarose gel electrophoresis. A clone was isolated that encoded approximately 48 repeats of the elastic sequence **B**. Plasmid pB9 encoded the triblock copolymer protein **B9** as a single contiguous reading frame within plasmid pET-24a (Scheme 2).

Scheme 2. Amino Acid Sequence of Protein-Based Block Copolymers B9 and P2 Derived from Concatemerization of Elastin-Mimetic Peptide Sequences A and B

{VPAVG[(IPAVG)$_4$(VPAVG)]$_{16}$IPAVG}-[X]-{VPAVG[(IPAVG)$_4$(VPAVG)]$_{16}$IPAVG}

B9 [X] = VPGVG[(VPGVG)$_2$VPGEG(VPGVG)$_2$]$_{48}$VPGVG

P2 [X] = VPGVGVPGVG

Plasmids pP2 and pB9 were used to transform the *E. coli* expression strain BL21-Gold(DE3). Large-scale fermentation

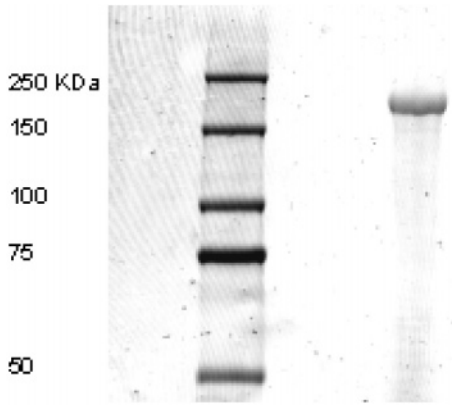

Figure 1. Sodium dodecyl sulfate−polyacrylamide gel electrophoresis (SDS−PAGE) analysis of **B9** protein copolymer. **B9** was run on 7.5% SDS−PAGE and stained with Coomassie G250 (Bio-Rad). Molecular weight markers werePrecision Plus Protein Kaleidoscope (Bio-Rad).

(3L) was performed at 37 °C in Terrific Broth (TB) medium supplemented with kanamycin (50 μg/mL).[6] The fermentation cultures were incubated under antibiotic selection for 36−48 h at 37 °C with agitation at 175 rpm in an orbital shaker. Cells were harvested via centrifugation at 4 °C and 4000*g* for 20 min, and the cell pellet was resuspended in lysis buffer (150 mL; 100 mM NaCl, 50 mM Tris-HCl, pH 8.0) and stored at −80 °C. The frozen cells were lysed by three freeze/thaw cycles. Lysozyme (1 mg/mL), protease inhibitor cocktail (5 mL), benzonase (25 units/mL), and $MgCl_2$ (1 mM) were added to the lysate, and the mixture was incubated at 25 °C for 30 min. The cell lysate was incubated for 12 h at 4 °C and was centrifuged at 19 000*g* for 30 min at 4 °C to pellet the cell debris. The target proteins were purified from the clarified cell lysate by three to five cycles of temperature-induced precipitation (4 °C/37 °C) from 500 mM NaCl solution. Dialysis and lyophilization afforded proteins **B9** and **P2** as fibrous solids in isolated yields of 418 mg/L of culture and 781 mg/L of culture, respectively.

Amino Acid Compositional Analysis. B9. Calcd (mol %): Ala, 8.1; Glx, 2.4; Gly, 31.9; Ile, 6.4; Pro, 20.0; Val, 31.2. Obsd (mol %): Ala, 10.8; Glx, 2.0; Gly, 28.3; Ile, 7.0; Pro, 22.8; Val, 28.2. **P2**. Calcd (mol %): Ala, 19.8; Gly, 20.2; Ile, 15.7; Pro, 20.0; Val, 24.3. Obsd (mol %): Ala, 19.7; Gly, 20.1; Ile, 14.9; Pro, 21.6; Val, 23.7. MALDI−TOF mass spectrometry: Obsd (Calcd): **B9**, 165, 356 (165, 564); **P2**, 72, 016 (72, 116). Sodium dodecyl sulfate−polyacrylamide gel electrophoresis (SDS-PAGE) analysis indicated apparent molar masses of approximately 180 000 Da for **B9** (Figure 1). ^{1}H NMR and ^{13}C NMR spectra for **B9** and **P2** were measured at 4 °C, and chemical shifts were reported relative to the internal sodium 2,2-dimethyl-2-silapenta-5-sulfonate (DSS) (Tables 2 and 3).

Differential Scanning Calorimetry. All DSC measurements were conducted on a CSC Nano II differential scanning calorimeter (N-DSC II) at a protein concentration of 1 mg/mL and a scan rate of 1 °C/min. Distilled deionized water was used as a solvent in all cases. The thermograms were corrected for instrumental baseline by obtaining the DSC trace of the pure solvent. The transition temperatures and heats of transition were computed using the *cpcalc* analysis software provided with the instrument.

Tensile Measurements. Films of the homopolymer **P2** and the triblock copolymer **B9** were cast from 10 wt % solutions in TFE and water. Although protein solutions were prepared at 5 °C, solvent evaporation was performed at either 5 or at 23 °C. Since it is known that fluorinated alcohols form strong solid-state complexes with polyamides,[7] thermogravimetric analysis (TGA) was conducted on dried films to verify complete removal of solvent from films samples. TGA showed no weight loss up to degradation. Given the sensitivity of TGA, this indicates that residual solvent, even if present, was below 0.05 wt %. After complete solvent evaporation, films were hydrated in a phosphate buffer saline (pH 7.4), cut into 5 mm × 15 mm strips for tensile analysis, and stored in PBS for a further 24 h prior to tensile testing. Hydrated film thickness was measured by optical microscopy using a standard image analysis protocol.

A miniature materials tester Minimat 2000 (Rheometric Scientific) was used to determine the mechanical film properties in the tensile deformation mode with a 20 N load cell, a strain rate of 5 mm/min, and a gauge length of 5 mm. Tensile testing was conducted at room temperature and ambient relative humidity. Eight to ten specimens were tested, and the average Young's modulus, tensile strength, and elongation to break were determined. Hysteresis measurements were performed at a strain rate of 5 mm/min in both the loading and unloading directions.

Table 2. Sequential Residue Assignments for Polypeptide B9 Derived from ^{1}H NMR and ^{13}C NMR Spectroscopic Data Measured at 4 °C[a]

residue	NH (ppm)	αH (ppm)	βH (ppm)	other (ppm)
Val[1]	8.05	4.54	2.1	γCH_3 0.97, 0.92
Ile[1]	8.35	4.52	1.9	γCH_2 1.46, 1.10; γCH_3 0.97; δCH_3 0.92
Pro[2]		4.5	2.31, 1.95	γCH_2 2.01, 2.01; δCH_2 3.70, 3.90
Gly[3]	8.47	4.0		
Ala[3]	8.65	4.8	1.40	
Val[4]	8.00	4.38	2.1	γCH_3 0.97, 0.92
Glu[4]	8.34	4.30	2.06, 1.96	γCH_2 2.36, 2.36
Gly[5]	8.53	4.10		

residue	C=O (ppm)	αC (ppm)	βC (ppm)	other (ppm)
Val[1]	174.6	60.5	32.6	γCH_3 20.9, 20.9
Ile[1]	174.4	59.5	39.0	γCH_2 28.0; γCH_3 17.1; δCH_3 13.5
Pro[2]	177.4	64.0	33.0, 33.5	γCH_2 28.0; δCH_2 51.5
Gly[3]	173.5	45.5		
Ala[3]	177.6	53.5	20.0	
Val[4]	176.6	63.0	32.6	γCH_3 20.9, 20.9
Glu[4]	176.1	56.6	30.1	γCH_2 37.0; δCO 183.9
Gly[5]	174.0	45.5		

[a] Chemical shifts are referenced and reported relative to the internal sodium 2,2-dimethyl-2-silapenta-5-sulfonate (DSS).

Table 3. Sequential Residue Assignments for Polypeptide P2 Derived from ^{1}H NMR and ^{13}C NMR Spectroscopic Data Measured at 4 °C[a]

residue	NH (ppm)	αH (ppm)	βH (ppm)	other (ppm)
Val[1]	8.05	4.54	2.1	γCH_3 0.97, 0.92
Ile[1]	8.35	4.52	1.9	γCH_2 1.46, 1.10; γCH_3 0.97; δCH_3 0.92
Pro[2]		4.5	2.31, 1.95	γCH_2 2.01, 2.01; δCH_2 3.70, 3.90
Gly[3]	8.47	4.0		
Ala[3]	8.65	4.8	1.40	
Val[4]	8.00	4.38	2.1	γCH_3 0.97, 0.92
Gly[5]	8.53	4.10		

residue	C=O (ppm)	αC (ppm)	βC (ppm)	other (ppm)
Val[1]	174.6	60.5	32.6	γCH_3 20.9, 20.9
Ile[1]	174.4	59.5	39.0	γCH_2 28.0; γCH_3 17.1; δCH_3 13.5
Pro[2]	177.4	64.0	33.0, 33.5	γCH_2 28.0; δCH_2 51.5
Gly[3]	173.5	45.5		
Ala[3]	177.6	53.5	20.0	
Val[4]	176.6	63.0	32.6	γCH_3 20.9, 20.9
Gly[5]	174.0	45.5		

[a] Chemical shifts are referenced and reported relative to internal sodium 2,2-dimethyl-2-silapenta-5-sulfonate (DSS).

Rheology. Rheological data was measured using a DMTA V (Rheometric Scientific) in the tensile mode. The data were collected with samples immersed in PBS at 23 °C. Storage modulus (E'), loss modulus (E''), and tan δ (E''/E') were measured at a strain of 0.5% in the frequency range of 0.5−10 Hz.

Cryo-HRSEM. PBS hydrated films were plunged into liquid ethane at its melting point (−183 °C), and the vitrified samples were stored in liquid nitrogen (LN2). Samples were transferred to and mounted on the precooled (ca. −170 °C) Oxford CT-3500 cryo-stage held in the cryo-preparation chamber. Specimens were fractured with a prechilled blade and washed with LN2. The shutters on the stage were closed to minimize frost contamination, and the cryo-stage was transferred to the Denton DV-602 Cr coater. To remove excess water (vitreous ice), the stage was allowed to equilibrate in a vacuum of $\sim 10^{-7}$ Torr. Shutters were then opened, and the stage was brought to a temperature of −105 °C for varying time intervals. The stage shutters were closed, and the stage was returned to −170 °C. A monatomic (1 nm) film of chromium was sputter-coated onto the specimen, and the stage was transferred to the upper stage of the DS-130F field-emission SEM operated at 25 kV. During the imaging process, specimen temperature was maintained at −115 °C. Images were digitally collected (5 MB) in 16 s in order to reduce radiation damage.

Solid-State ^{1}H NMR Spectroscopy. B9 films initially cast from TFE or water were packed in 4 mm rotors and rehydrated by immersion in deuterated PBS for 36 h at room temperature. ^{1}H solid-state NMR experiments were performed on a Bruker DSX400 NMR spectrometer operating at a magnetic field of 9.4 T. Samples were investigated at room temperature (295 K) in a conventional CP-MAS probe at a spinning speed of 5 kHz. CPMG relaxation experiments were performed using a train of π-pulses at a length of ca. 10 μs separated by a time interval of 200 μs.[8]

The instrumentation and methodology for conducting static NMR experiments at well-defined levels of relative humidity (RH) and material moisture content have been detailed elsewhere.[9] Samples were exposed to a humid environment by inserting a small amount of pure D_2O or D_2O saturated with sodium chloride at the bottom of a standard 5 mm NMR tube. Approximately 20 mg of **B9** film was placed on a plug of glass fibers, such that the sample and the glass fiber plug were not in direct contact with the humidifying fluid. NMR tubes were sealed and stored at 22 °C, leading to relative humidities of ca. 75% for the saturated NaCl solution and ca. 95% for the pure D_2O. Film moisture content was determined in a separate experiment using a gravimetric moisture sorption balance (IGASorp, Hidden Analytical, Warrington, UK). NMR data were recorded after 48 h, and further exposure time did not lead to measurable differences in results. Hahn echo experiments were performed using a ^{1}H broadband probe with a 5 mm coil insert achieving a 90° pulse length of ca. 7 μs. The NMR tube was inserted into the coil so that only the sample was within the active volume of the coil.

T_2 relaxation constants, measured using the CPMG sequence under conditions of MAS or the Hahn echo sequence under static conditions, were determined by fitting data sets to eq 1 using the software package IGOR PRO (Wavemetrics, Lake Oswego, OR).

Elution of a Model Amphiphilic Drug. Sphingosine-1-phosphate (S1P; MW 378) contains a C16 alkyl chain and a zwitterionic headgroup, containing both amino and phosphate moieties, and was used as a model amphiphilic drug to assess the influence of triblock microstructure on drug release rates. A total of 2 mg of S1P was added to 1 mL of a 10 wt % solution of **B9** (100 mg) in either TFE or water. Films of equivalent dimension were cast at room temperature and casting solvent allowed to evaporate until films were completely dry. Films were then rehydrated in PBS at 37 °C, and release of S1P was assessed by UV−vis spectroscopy. Release rates were normalized to total S1P content, which was verified by intentional film dissolution at 4 °C at the end of the elution period.

Results and Discussion

Synthesis of Diblock and Triblock Protein Copolymers. Prior studies by Urry and colleagues[10,11] have noted that the phase behavior and mechanical properties of elastin-mimetic polypeptides depend critically on the identity of the residues within the pentapeptide repeat sequence [(Val/Ile)-Pro-Xaa-Yaa-Gly]. Alterations in the identity of the fourth residue (Yaa) modulates the position of the inverse temperature transition (Tt) of the polypeptide in aqueous solution in a manner commensurate with the effect of the polarity of the amino acid side chain on polymer−solvent interactions. Specifically, increasing the polarity of this residue raises the temperature at which the protein coacervates. In addition, these investigators also observed that in hydrated, radiation cross-linked materials substitution of an Ala for the consensus Gly residue in the third (Xaa) position of the repeat sequence changed the mechanical response of the material from elastic to plastic deformation. This effect was attributed to a change from a type II to a type I β turn upon substitution of Pro-Gly with Pro-Ala in the pentapeptide repeat sequence. These observations established a framework for our design of a new class of protein triblock copolymers that mimic thermoplastic elastomers. Specifically, an amphiphilic polypeptide was expressed that incorporates identical *end blocks* of a *hydrophobic plastic sequence* $[(IPAVG)_4(VPAVG)]_n$ separated by a *central hydrophilic elastomeric block* $[(VPGVG)_4(VPGEG)]_m$ (Scheme 2). The repeat sequence of the end blocks was chosen such that their inverse temperature transition would reside at or near ambient temperature (~20 °C), which would result in phase separation of the hydrophobic domains from aqueous solution under physiologically relevant conditions (pH 7.4, T 37 °C). In turn, the sequence of the central elastomeric repeat unit was chosen such that its transition temperature was significantly higher than 37 °C.

Two target protein polymers were synthesized: a diblock consisting of flanking plastic end blocks, designated as **P2**, and the corresponding triblock with a central elastomeric block, designated as **B9** (Schemes 1 and 2). Isolated yields for **B9** and **P2** were 418 mg/L of culture and 781 mg/L of culture, respectively. Amino acid analysis confirmed the expected composition for both protein polymers, and mass spectrometry verified anticipated molar masses of 165 and 72 kDa for **B9** and **P2**, respectively. The inverse temperature transition was 13 °C for **P2** and 15 °C for **B9**. While the capacity of both plastic and elastomeric blocks to coacervate under appropriate conditions was predictable, the ability of the chosen end block sequence to form effective *virtual* cross-linking sites and to retain plastic deformation behavior in the absence of chemical or radiation cross-linking was completely unanticipated. Nonetheless, as illustrated by the investigations described below, the triblock protein polymer **B9** did indeed reversibly self-assemble from concentrated aqueous solution above the phase transition temperature of the hydrophobic end block to form a network of plastic microdomains dispersed in a continuous phase of the elastomeric midblock. It bears comment that inflammatory or allergic reactions have not been reported in response to related elastin protein polymers composed of similar peptide sequences, including VPGVG, VPGKG, VPGEG, IPAVG, and VPAVG.[12] In addition, these peptide sequences do

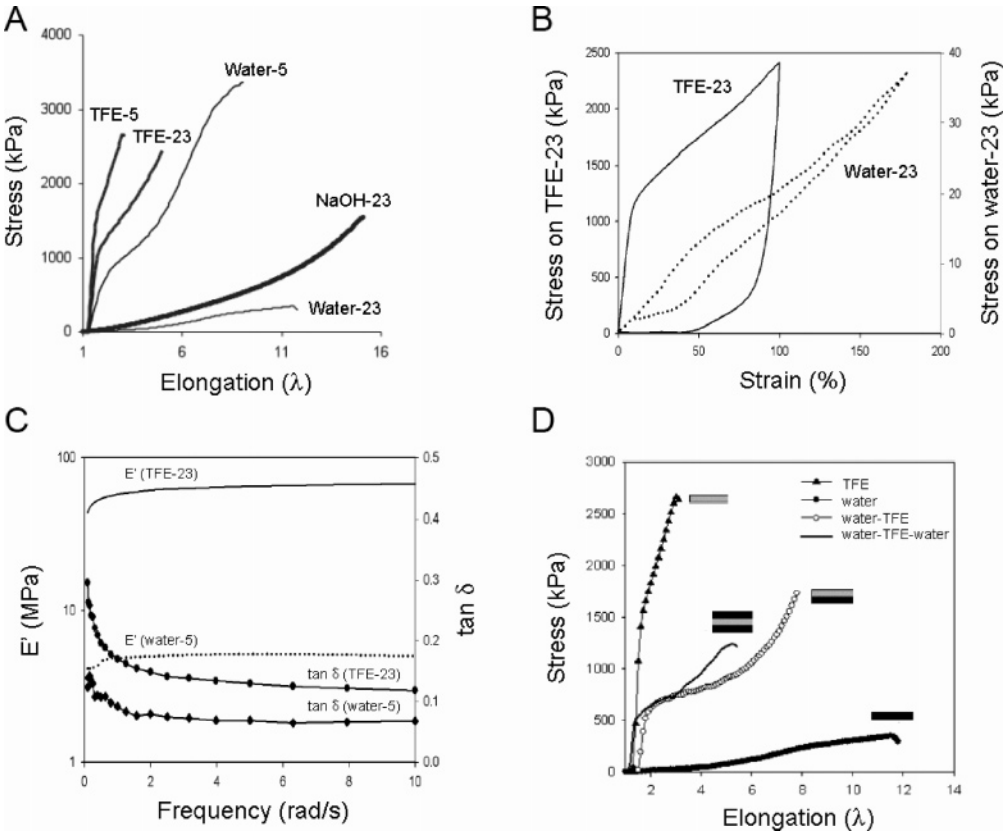

Figure 2. (A) Stress−strain curves for the **B9** triblock copolymer cast at different temperatures from water or TFE. TFE solvates both blocks and renders the material plastic, while water as a preferential solvent for the hydrophilic midblock generates an elastomeric material. Changing the pH of the solvent by addition of NaOH further enhances the elastic properties. Elongation λ represents (strained length)/(initial length). (B) Hysteresis curves for **B9** cast from TFE and water. Mechanical hysteresis is noticeably reduced in samples cast from water at 23 °C compared to samples cast from TFE at 23 °C, demonstrating that water-cast samples are more elastic. (C) Dynamic mechanical data for **B9** cast from water or TFE. The tan δ for both samples are similar indicating comparable losses due to viscous dissipation. (D) Stress−strain curves for the **B9** cast as multilamellar films from water or TFE at room temperature and subsequently hydrated in PBS at 23 °C.

not appear to be chemotactic to leukocytes, in contrast to other elastin degradation products.[13,14]

Mechanical Behavior and Viscoelastic Properties of Protein Triblock Copolymer Films. When a block copolymer solidifies from solution, the resulting microstructure is dictated by the presence or absence of phase transitions in the polymer solution and domain mixing or microphase separation within the polymer rich phase.[15−18] Both processes are influenced by solvent−polymer and polymer−polymer interactions and have important implications for practical applications employing block copolymers. For example, phase transitions or liquid−liquid phase separation (LLPS) have been utilized to generate spherical particles as well as microporous materials with bicontinuous, closed-cell, or open-cell morphologies. Likewise, the degree of interphase or domain mixing that occur during the processing of synthetic block copolymers effects nanoscale structure that has been shown to influence material properties as diverse as mechanical behavior, material stability, and gas permeability.

The potential of solvent processing to dramatically influence the mechanical properties of this class of protein based block copolymer is illustrated by the engineering stress−strain curves and the corresponding tensile data obtained for the homopolymer **P2** and triblock **B9** samples when initially cast from TFE or water and subsequently evaluated at room temperature after hydration in PBS (Figure 2A, Table 2). **P2**, whether cast from TFE or water, displays tensile behavior similar to materials exhibiting plastic or irrecoverable deformation under stress with a Young's modulus for hydrated **P2** films that ranged between 16 and 55 MPa. Since TFE is a good solvent for both hydrophobic and hydrophilic blocks of **B9**, film casting from TFE was expected to produce a material with significant interpenetration of both blocks and, as a result, yield a microstructure characterized by a mixed interface between both domains upon solvent removal. Although subsequent rehydration of the solvent-processed material in PBS at temperatures greater than 20 °C would induce end block aggregation and consequent phase separation, some portion of the end block would remain kinetically trapped within the soft midblock segments. In this regard, previous investigations of synthetic thermoplastic elastomers, such as SBS or SIS copolymers, have demonstrated that solvent-induced interphase mixing of incompatible polystyrene and polyolefin domains affords materials that show plastic deformation under stress with tensile properties resembling those of the plastic polystyrene block.[19,20] Indeed, the stress−strain curve of hydrated **B9** is qualitatively similar to that of **P2**, when both are initially cast from TFE. These data suggest that the

sustained load is largely carried by plasticlike [$(IPAVG)_4$-(VPAVG)] domains that extend over relatively long regions of the material, likely as cylindrical or lamellar microstructures. Thus, the behavior of **B9** cast from TFE can be likened to a rubber-toughened version of **P2**. Tensile properties of **B9** films cast from TFE at 5 and 23 °C remained similar since TFE is a good solvent for **B9** at both temperatures.

Unlike TFE, water can be viewed as a selective solvent, preferentially solvating the hydrophilic midblock more than the hydrophobic end blocks. Limited mixing at the interface of these two incompatible domains would be anticipated in films cast from water. Thus, subsequent rehydration of water cast films in PBS would be expected to produce a material with a sharper interface between plastic and elastomeric domains than for films cast from TFE. In turn, this would reduce the participation of the end blocks in the tensile deformation process, thereby enhancing material elasticity (Figure 2A). Of note, the tensile behavior shown by water-cast samples is qualitatively similar to that observed for SBS copolymers cast from solvents that preferentially solvate the butadiene block.[19,20] Increasing the solvent casting temperature from 5 °C to 23 °C further favors end block aggregation, since this temperature lies above the transition temperature of the end block. The result is a true microphase-separated material in which there are likely spherical islands of hydrophobic end blocks dispersed among solvent swollen and conformationally labile midblock chains. Owing to almost complete nonparticipation of the end blocks in the tensile deformation process, this material is truly elastic with an observed elongation to break in the range of 1000%. Consistent with these observations, hysteresis is significantly greater in TFE-cast samples as compared to the more elastomeric water-cast films produced at 23 °C (Figure 2B).

Dynamic mechanical testing provided further insight into mechanical property differences observed as a function of film processing conditions (Figure 2C). While the elastic or storage modulus (E′) of the TFE-cast sample is much greater than that of the sample cast from water below the transition temperature, the tan δ for both samples are similar. Tan δ is the ratio of the loss modulus (E″) to storage or elastic modulus (E′) of a material. As such, losses due to viscous dissipation are similar in both samples providing further support that factors which promote block mixing, including the use of a non-selective solvent or casting from a selective solvent below the transition temperature lead to similar viscous-like responses.

Since the midblock contains glutamic acid residues, further modulation of domain mixing can be expected during material processing as a function of solution pH. Samples of **B9** cast from a 0.1 N NaOH solution (pH 14) at 23 °C and subsequently rehydrated in PBS proved to be more elastic than comparable samples cast from water at 23 °C (Figure 2A, Table 4). In a highly basic solution, the glutamic acid residues will reside in an ionized state (COO^-) since their pK_a is ~4. This will contribute to a greater degree of midblock swelling due to charge−charge repulsions and further accentuates the incompatibility of the two domains. Indeed, the loss modulus for samples cast from NaOH was lower than that observed for water-cast samples (data not shown), demonstrating a further augmentation of elastic behavior. Remarkably, under these conditions maximum elongation to break exceeded 1300%, which is a value approximately 3−13 times greater than observed among other covalently crosslinked recombinant elastomeric biosolids.[21] Of interest, the capacity to further modulate mechanical properties by generating composite layered films of alternating TFE and water cast lamellae has also been demonstrated (Figure 2D).

Table 4. Tensile Parameters for P2 and B9 Films Cast from TFE and Water

sample[a]	modulus (MPa)	tensile strength (MPa)	elongation to break (%)
P2 (water-5)	16.65 ± 1.55	3.00 ± 0.32	128 ± 33
P2 (TFE-5)	55.04 ± 11.89	5.59 ± 1.01	152 ± 42
B9 (TFE-5)	17.8 ± 1.7	2.70 ± 0.40	390 ± 53
B9 (TFE-23)	35.26 ± 2.83	2.28 ± 0.58	250 ± 47
B9 (water-5)	1.3 ± 0.29	2.87 ± 0.88	640 ± 116
B9 (water-23)	0.03 ± 0.01	0.78 ± 0.28	1084 ± 67
B9 (NaOH-23)	0.03 ± 0.006	1.24 ± 0.29	1330 ± 64

[a] Water-5, water-23, TFE-5, TFE-23, and NaOH-23 refer to casting solvent and temperature in °C.

High-Resolution Cryo-Scanning Electron Microscopy of Protein Copolymer Films. When a polymer solidifies directly from solution, the resulting mesoscopic morphology depends on whether liquid−liquid phase separation (LLPS) precedes polymer solidification. Moreover, the scale on which LLPS-dictated morphology occurs is determined by the nature of the phase transition and, in particular, whether spinodal or binodal decomposition occurs, with nucleation of either polymer- or solvent-rich phases. Characteristically, nucleation of the polymer-rich phase yields globular structures that are on a smaller length scale (0.01−0.1 μm) than the cells that arise through nucleation of the solvent-rich phase (1−10 μm) due to the much slower diffusion rates associated with the former process. The mesoscopic morphology of PBS hydrated **B9** films initially cast from either water or TFE was examined by cryo-high-resolution scanning electron microscopy (cryo-HRSEM). Although all films were microporous, remarkable processing-dependent differences were noted (Figures 3 and 4). Specifically, protein triblock films cast from water at 23 °C displayed an open cell morphology (pore diameter ca. 500 nm), while those cast from TFE were characterized by the spontaneous formation of highly aligned fiber networks (fiber diameter ca. 200 nm). Thus, we speculate that the open cell morphology exhibited by water cast samples was probably a result of initial nucleation of solvent-rich phases during LLPS. In contrast, it appears likely that the fiber-based morphology observed within TFE cast films was due to the initial nucleation of polymer-rich phases during LLPS with subsequent coalescence of nucleating sites. Commensurate with differences in mesoscopic morphology, water content differed substantially among these materials. Water sorption was 695 ± 63% (mean ± SD; (w/w)) for films cast from water at 23 °C, compared with 258 ± 59% for those samples cast from TFE.

Solid-State ^{1}H NMR Spectroscopy of Protein Copolymer Films. Solid-state ^{1}H NMR spectroscopy was used to study the nanoscale features of cast polymer films. NMR experiments were conducted under magic angle spinning (MAS) for **B9** films cast from TFE and water at 23 °C and subsequently hydrated in deuterated PBS (Figure 5A). The measured spectra consist of a broad spinning-sideband pattern with a spectral width

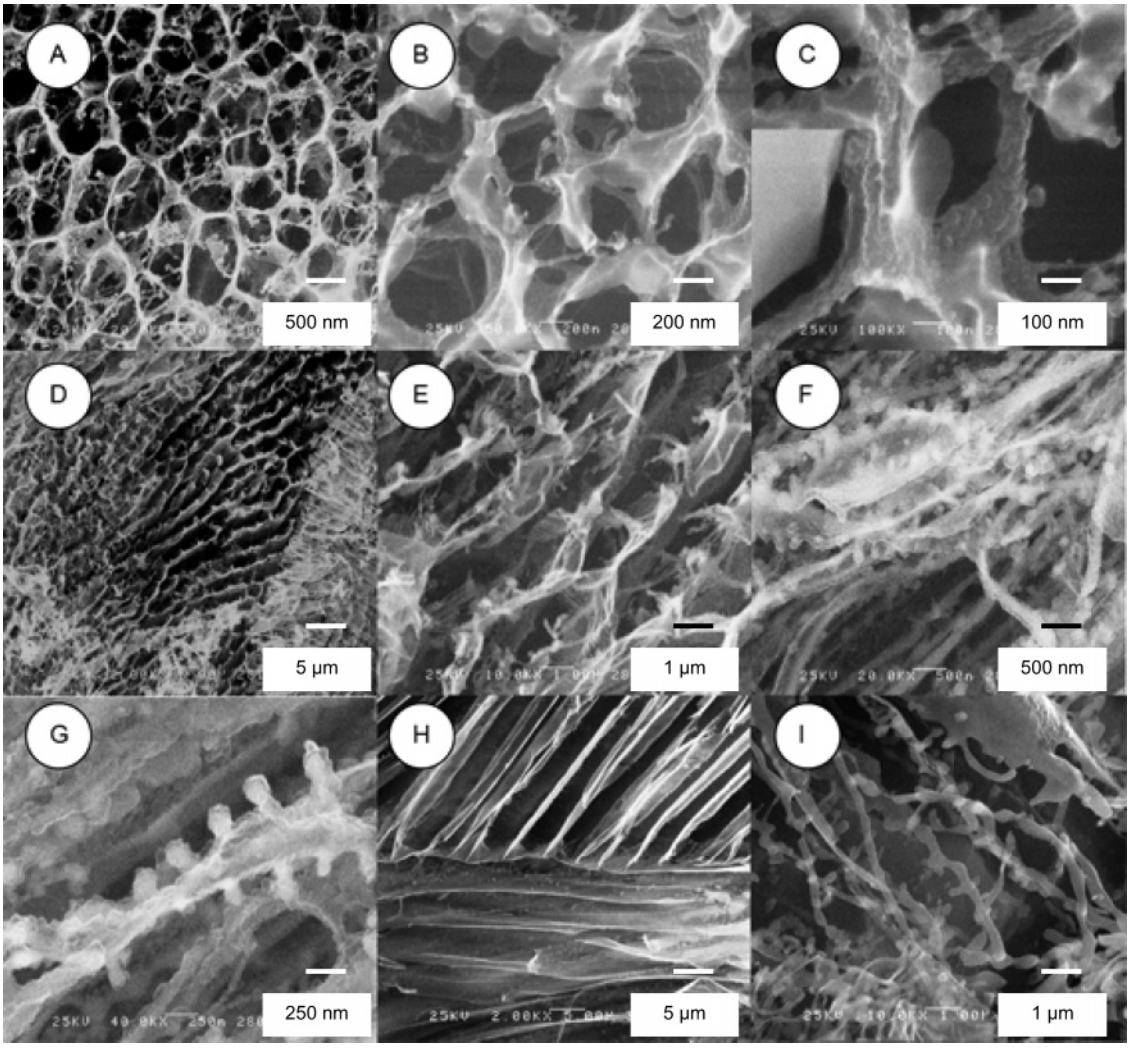

Figure 3. Cryo-HRSEM micrographs of **B9** rehydrated in PBS after initial room temperature casting from water (A−C) and TFE (D−G) and cold room casting from water (H−I). The open cell morphology exhibited by room temperature water-cast samples suggests initial nucleation of solvent-rich phases during LLPS. In contrast, the fiber-based morphology observed in TFE-cast films is consistent with initial nucleation of polymer-rich phases during LLPS with subsequent coalescence of nucleating sites.

exceeding 50 kHz. Superimposed on this pattern is a narrow spectrum (less than 10 ppm in spectral width), which exhibits several peaks distinguishable by their chemical shift. The data in Figure 5A are scaled to display only that potion of the spectrum corresponding to mobile polymer chains. The broad spectral feature, which is not visible in Figure 5A, corresponds to rigid, immobile polymer components. For both samples the spectra of mobile components reflect identical chemical structure. However, the peaks for TFE cast films were significantly broader than those cast from water. These observations are consistent with a reduction in polymer chain mobility in protein films cast from TFE. Relative molecular mobilities for both protein polymer chains and the associated water component were quantitatively characterized by measuring T_2 spin−spin relaxation values through a Carr−Purcell−Meiboom−Gill (CPMG) experiment.[8] Specifically, the observed relaxation behavior was fit to the biexponential relaxation function

$$I(TE) = w_a \exp\left\{-\frac{TE}{T_{2a}}\right\} + w_b \exp\left\{-\frac{TE}{T_{2b}}\right\} + w_c \quad (1)$$

where I is the peak intensity measured as a function of the relaxation delay (TE) and T_{2a} and T_{2b} are respective relaxation constants for proton fractions weighted by the factors w_a and w_b (Figure 5B). The parameter w_c accounts for any offset in measured peak intensity and did not contribute significantly to the fit of CPMG data. Although eq 1 represents only one of several possibilities that may be used to describe the complex relaxation data, it provides a simple and effective method for quantitative data comparison. As suggested by the broad line widths in Figure 5A, **B9** films cast from TFE exhibited lower values for T_{2a} and T_{2b}, which indicates decreased molecular motion when compared with water cast **B9** films (Table 5).

The molecular mobilities of polymer chains can generally be related to the degree of polymer plasticization and in turn correlated with material mechanical properties. Indeed, T_2 relaxation times for fully hydrated samples reflect results obtained from mechanical testing. Commensurate with smaller T_2 relaxation times and reduced polymer chain mobility, the Young's modulus and tensile strength are greater and the elongation to break smaller for films cast from TFE. While it might be presumed that variations in mechanical behavior can be attributed to differences in the amount of water in a given film, solid-state NMR analysis conducted under conditions of controlled moisture content revealed that

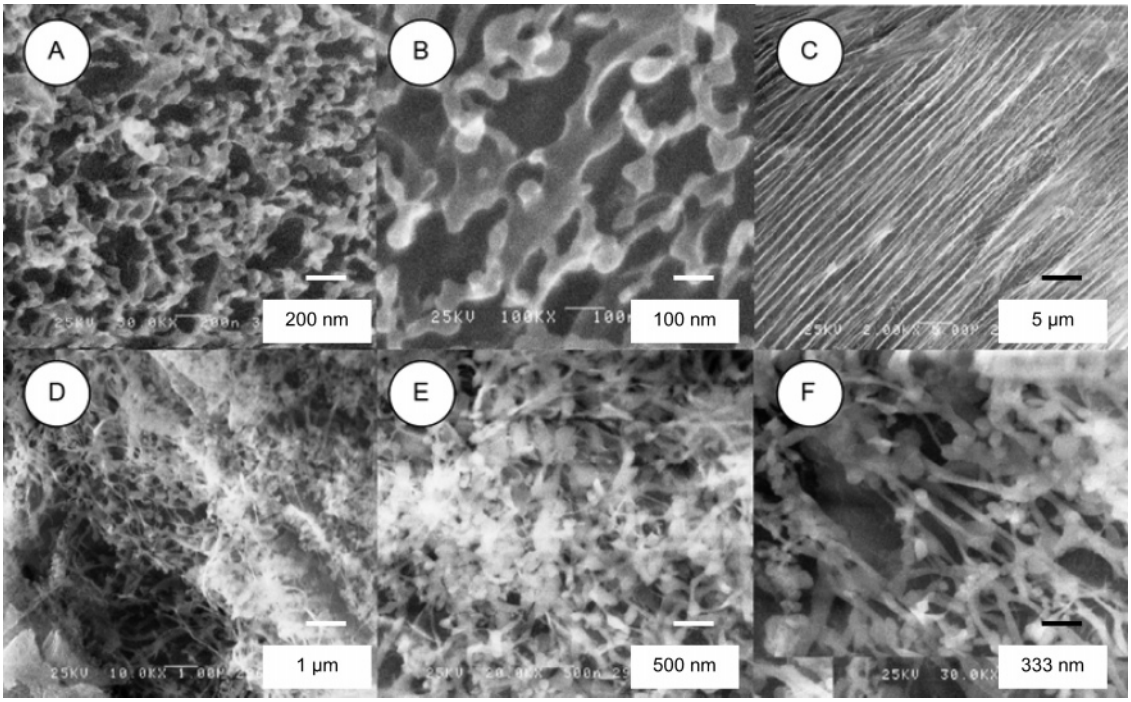

Figure 4. Cryo-HRSEM micrographs of **P2** rehydrated in PBS after initial room temperature casting from water (A−B) and TFE (C−F).

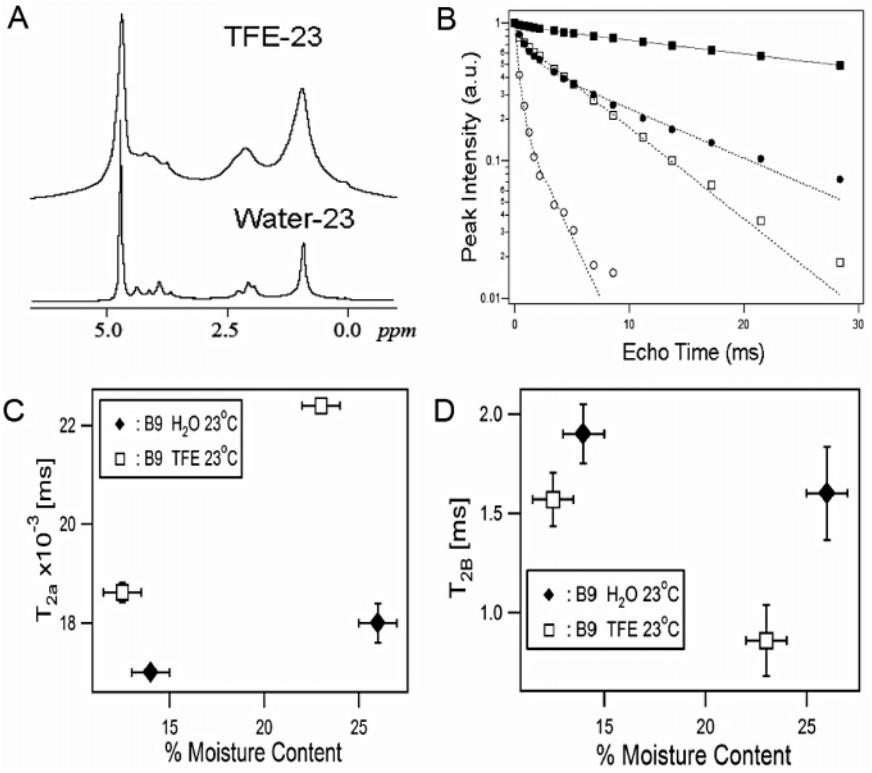

Figure 5. (A) ^{1}H NMR MAS spectra of B9 films cast from TFE or water after rehydration in deuterated PBS (only central part of the spectrum is shown). (B) T_2 relaxation curves measured for B9 cast from water (■, water peak; ●, aliphatic peak) or TFE (□, water peak; ○, aliphatic peak). Dashed lines represent least-squares fits to eq 1. T_{2a} (C) and T_{2b} (D) relaxation constants for TFE and water cast B9 films of defined water content.

film-specific mechanical behavior is largely due to unique processing-induced nanoscopic features. Specifically, T_2 relaxation constants were determined from a Hahn echo analysis[22] of static solid-state ^{1}H NMR data acquired under conditions of controlled relative humidity.[9] This technique is especially suited to study T_2 relaxation at very short time delays (TE), which is required to characterize the relaxation of rigid polymer chains. Data corresponding to total proton contents were regressed to eq 1. A good fit was only achieved by accounting for w_c, which represents a highly mobile fraction of plasticized components with T_2 relaxation times that are larger than a few milliseconds. Hence, the mobile components, previously detected in the CPMG experiment under conditions of MAS, are now accounted by T_{2b} and $w_{b,c}$. In contrast, the short

Table 5. T_2 Relaxation Data for Hydrated B9 Films Cast from TFE and Water

	w_a	T_{2a} [ms]	w_b	T_{2b} [ms]
B9 TFE-23				
4.7 ppm (water)	0.80 ± 0.01	6.5 ± 0.1	0.20 ± 0.01	0.3 ± 0.05
1.0 ppm (methyl)	0.21 ± 0.03	2.4 ± 0.4	0.78 ± 0.03	0.4 ± 0.05
B9 water-23				
4.7 ppm (water)	0.94 ± 0.003	43.4 ± 0.4	0.05 ± 0.01	1.3 ± 0.2
1.0 ppm (methyl)	0.54 ± 0.02	12.1 ± 0.6	0.45 ± 0.02	1.1 ± 0.1

relaxation time T_{2a} represents the rigid fraction. If TFE and water cast samples exhibited identical nanostructure, all data points measured at different moisture contents for T_{2a} or T_{2b} would be defined by a continuously increasing function. Figure 5C,D demonstrates that this is not the case, which supports the notion that processing conditions induce distinct microdomain morphologies. Notably, T_{2a} (rigid domains) is smaller and T_{2b} (plasticized domains) is larger for water cast **B9** films when compared to respective relaxation constants observed for **B9** films cast from TFE. This indicates that **B9** films prepared from water exhibit decreased polymer chain mobility in the rigid phase and increased mobility in the mobile phase. Considering the triblock structure of the protein polymer, these data confirm that a sharper interface exists between plastic- and elastic-like domains for water cast films when compared to those produced from TFE. All told, the presence of a diffuse interface in TFE cast samples can only be attributed to the presence of intermixing between plastic- and elastic-like domains. The sample cast from TFE exhibits a higher value of T_{2a} and a lower value of T_{2b} when compared to the sample cast from water. The presence of a significant interphase between rigid and mobile phases is not taken into account by eq 1, but it is obvious that the closer proximity between values T_{2a} and T_{2b} reflect a more continuous transition between rigid and mobile phases within the sample cast from TFE. These data confirm that while the presence of water is necessary for displaying plastic and elastic responses, the degree of plasticization and its related effect on polymer chain mobility and film properties, such as material mechanical behavior, is largely a consequence of the nanoscale geometry of the triblock domains. The combination of highly plasticized midblocks in association with discrete and relatively rigid, microphase-separated plastic-like domains appears responsible for the remarkable level of observed elasticity and extensibility in water cast samples. These responses exceed those of previously reported virtually crosslinked thermoplastic elastomers, produced by either traditional chemical or biosynthetic approaches and examined as single-component materials.

Release Rates of a Model Amphiphilic Drug from Protein Triblock Copolymer Films. Commensurate with differences in mesoscopic morphology and microphase separation, drug elution profiles also differed substantially among these materials and provides a second example of the capacity of processing conditions to tune properties of triblock protein polymers. The release rate of amphiphilic drugs from amphiphilic block copolymers is directly related to the degree of mixing of hydrophilic and hydrophobic blocks. For example, under identical drug loading conditions the diffusion coefficient of the EDG-receptor agonist, sphingosine-1-phosphate (S1P), which contains both a C16 alkyl chain and a zwitterionic headgroup, was 30-fold higher from water cast films of **B9** than from those produced from TFE (2.33×10^{-7} cm^2/s vs 7.87×10^{-9} cm^2/s) (Figure 6). Presumably, this difference is due to substantial interdomain mixing present within TFE cast samples, which yields a large amphiphilic interface for S1P binding.

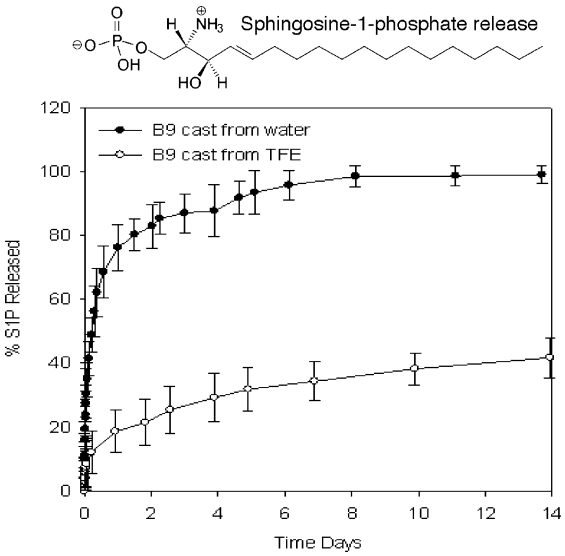

Figure 6. Elution profile in PBS at 37 °C of sphingosine-1-phosphate (S1P) from hydrated B9 films initially cast from water or TFE at room temperature. Calculated diffusion coefficients of S1P release from water- and TFE-cast films were 2.33×10^{-7} and 7.87×10^{-9} cm^2/s, respectively.

Conclusions

This report is the first to demonstrate the capacity to create recombinant protein-based thermoplastic elastomers that behave in a manner that is truly analogous to their nonprotein counterparts. In large measure, the development of this novel class of protein-based material was a consequence of a new biosynthetic design strategy that facilitates the synthesis of high molecular weight triblock copolymers comprised of large block sequences. Notably, enhanced control over both meso- and nanoscale structure was achieved by adopting simple processing approaches that influence liquid phase transitions during polymer solidification and interphase mixing between incompatible blocks. The ability to modulate these phenomena have not been previously noted in other protein polymer systems and provides an important mechanism for producing materials that exhibit a wide range of behavior, including mechanical properties and drug elution rates. We anticipate that protein-based thermoplastic elastomers will find applications as novel scaffolds for tissue engineering and as new biomaterials for controlled drug release and cell encapsulation. Significantly, this novel class of protein polymer illustrates important new design principles that are widely applicable to the generation of a variety of new recombinant protein-based materials with unique microstructures and properties.

Acknowledgment. This work was supported by grants from the NSF sponsored Georgia Tech/Emory ERC for the Engineering of Living Tissues as well as the NIH and NASA.

References and Notes

(1) Ferrari, F.; Cappello, J. In *Protein-Based Materials*; McGrath, K., Kaplan, D., Eds.; Birkhäuser: Boston, 1997.

(2) Petka, W. A.; Hardin, J. L.; McGrath, K. P.; Wirtz, D.; Tirrell, D. A. *Science* **1998**, *281*, 389.
(3) Cappello, J.; Crissman, J. W.; Crissman, M.; Ferrari, F. A.; Textor, G.; Wallis, O.; Whitledge, J. R.; Zhou, X.; Burman, D.; Aukerman, L., et al. *J. Controlled Release* **1998**, *53*, 105.
(4) (a) Legge, N. R., Holden, G., Schroeder, H. E., Eds. *Thermoplastic Elastomers*; Hanser: New York, 1987. (b) Alexandridis, P., Lindman, B., Eds.; *Amphiphilic Block Copolymers;* Elsevier: Amsterdam, 2000. (c) Spontak, R. J.; Patel, N. P. *Curr. Opin. Colloid Interface Sci.* **2000**, *5*, 334.
(5) (a) Wright, E. R.; McMillan, R. A.; Cooper, A.; Apkarian, R. P.; Conticello, V. P. *Adv. Funct. Mater.* **2002**, *12*, 149. (b) Wright, E. R.; Conticello, V. P. *Adv. Drug Deliv. Rev.* **2002**, *54*, 1057.
(6) Daniell, H.; Guda, C.; McPherson, D. T.; Zhang, X.; Xu, J.; Urry, D. W. *Methods Mol. Biol.* **1997**, *63*, 359.
(7) Sturgill, G. K.; Stanley, C.; Rezac, M. E.; Beckham, H. W. *Macromolecules* **2001**, *34*, 8730.
(8) Meiboom, S.; Gill, D. *Rev. Sci. Instrum.* **1958**, *29*, 688.
(9) Leisen, H.; Beckham, H. W.; Benham, M. *Solid State Nucl. Magn. Reson.* **2002**, *22*, 409.
(10) Urry, D. W. *J. Phys. Chem. B* **1997**, *101*, 11007.
(11) Urry, D. W.; Luan, C.-H.; Harris, C. M.; Parker, T. M. In *Protein-Based Materials*; McGrath, K., Kaplan, D., Eds.; Birkhäuser: Boston, 1997.
(12) Urry, D. W.; Pattanaik, A.; Accavitti, M. A.; Luan, C. X.; McPherson, D. T.; Xu, J.; et al. In *Handbook of Biodegradable Polymers*; Domb, A. J., Kost, J., Wiseman, D. M., Eds.; Harwood: Amsterdam, 1997; pp 367−86.
(13) Hauck, M.; Seres, I.; Kiss, I.; Saulnier, J.; Mohacsi, A.; Wallach, J.; et al. *Biochem. Mol. Biol. Int.* **1995**, *37*, 45.
(14) Fulop, T., Jr.; Jacob, M. P.; Khalil, A.; Wallach, J.; Robert, L. *Pathol. Biol.* **1998**, *46*, 497.
(15) Akki, R.; Desai, P.; Abhiraman, A. S. *J. Appl. Polym. Sci.* **1999**, *73*, 1343.
(16) Bulone, D.; Emanuele, A.; San Biagio, P. L. *Biophys. Chem.* **1999**, *77*, 1.
(17) Alexandridis, P.; Richard, J.; Spontak, R. J. *Curr. Opin. Colloid Interface Sci.* **1999**, *4*, 130.
(18) Cheng, S. Z. D.; Keller, A. *Annu. Rev. Mater. Sci.* **1998**, *28*, 533.
(19) Séguéla, R.; Prud'homme, J. *Macromolecules* **1978**, *11*, 1007.
(20) Wilkes, G. L.; Bagrodia, S.; Ophir, Z.; Emerson, J. A. *J. Appl. Phys.* **1978**, *49*, 5060.
(21) (a) Urry, D. W.; Okamoto, K.; Harris, R. D.; Hendrix, C. F.; Long, M. M. *Biochemistry* **1976**, *15*, 4083. (b) Nowatzki, P. J.; Tirrell, D. A. *Biomaterials* **2004**, *25*, 1261. (c) Bellingham, C. M.; Lillie, M. A.; Gosline, J. M.; Wright, G. M.; Starcher, B. C.; Bailey, A. J.; Woodhouse, K. A.; Keeley, F. W. *Biopolymers* **2003**, *70*, 445.
(22) Hahn, E. L. *Phys. Rev.* **1950**, *80*, 580.

MA0491199